

Aeolian Sands of the Temperate Boreal Zone (Northern Asia)

Nikolay Akulov *, Maria Rubtsova, Varvara Akulova, Yuriy Ryzhov and Maksim Smirnov 

Institute of the Earth's Crust SB RAS, Str. Lermontova, 128, 664033 Irkutsk, Russia; rubtsova83@inbox.ru (M.R.); akulova@crust.irk.ru (V.A.); ryv@crust.irk.ru (Y.R.); smv.38@mail.ru (M.S.)

* Correspondence: akulov@crust.irk.ru; Tel.: +7-902-560-2105

Abstract: This article is devoted to the study of the Quaternary aeolian sands of the boreal zone of north Asia. Using the example of the study reference sections of the Selenga Dauria (Western Transbaikalia), it was established that the activation of aeolian processes is determined by the complex interaction of natural and anthropogenic factors. Natural factors include neotectonic movements; wide distribution of alluvial and lacustrine-alluvial deposits; a sharply continental semi-arid climate; and forest-steppe and steppe vegetation. Among the anthropogenic factors, the leading ones are deforestation, plowing of land and construction of new settlements, roads and other line structures. The obtained radiocarbon dating of buried soils and coal from ancient fire pits indicates the activation of aeolian processes during the Holocene. The main sources for aeolian transport (winnowing) are sands located in the areas of river and lake beaches, floodplains and river terraces. Almost all aeolian sands of the boreal zone were formed as a result of short-range wind transport. They form mini-deserts unfixed by vegetation, with active aeolian processes, dunes, barchans and deflationary basins. Aeolian swells and blowout basins characterize aeolian landscapes weakly fixed by vegetation. It is noted that aeolian deposits of the boreal zone of north Asia, in contrast to similar sands of the subtropical and tropic zones, consist of coarser-grained material. Medium- and fine-grained sands dominate their composition, which is polymineral and well-sorted. In subtropical and tropical deserts, they are predominantly monomineral, fine and fine-grained. At the same time, mainly minerals that are unstable to weathering (feldspars, plagioclases, pyroxenes and amphiboles) represent the mineralogical composition of the studied aeolian sands. Weathering-resistant minerals dominate the sands of classical deserts: quartz, leucoxene, ilmenite, epidote, zircon, garnets, tourmaline, rutile and others. Modern aeolian landscapes are a unique natural formation for the boreal zone of north Asia and can be successfully used for the development of ecotourism.

Keywords: aeolian sand; parabolic dune; deflation; desertification; desert; Transbaikalia; northern Asia



Citation: Akulov, N.; Rubtsova, M.; Akulova, V.; Ryzhov, Y.; Smirnov, M. Aeolian Sands of the Temperate Boreal Zone (Northern Asia). *Quaternary* **2024**, *7*, 55. <https://doi.org/10.3390/quat7040055>

Academic Editor: David J. Lowe

Received: 26 July 2024

Revised: 13 November 2024

Accepted: 18 November 2024

Published: 5 December 2024



Copyright: © 2024 by the authors. Licensee MDPI, Basel, Switzerland. This article is an open access article distributed under the terms and conditions of the Creative Commons Attribution (CC BY) license (<https://creativecommons.org/licenses/by/4.0/>).

1. Introduction

Paradoxically, most of the world's deserts and desertification zones were formed within river, lake, sea and ocean coastlines. A region's sediment dynamics are functions of its hydrology and landscape and therefore are likely to be sensitive to future changes in climate. Material carried by the wind for many hundreds and thousands of kilometers is mixed with sediments of different genetic types, so the recognition of aeolian deposits is difficult in some places. This is due to the similarity of the physical nature of wind and water sediment transport (ripples, sedimentation, etc.). Intensive manifestation of aeolian processes leads to a noticeable restructuring of the landscape. The lithogenic base changes and is partially or completely disrupted, and an aeolian microrelief is formed. A complete or partial replacement of the natural vegetation cover occurs.

It has been a century since the famous geologist and geographer V.A. Obruchev made an expedition through northern Asia and first touched upon the problem of the aeolian sands of Selenga Dauria [1]. On the schematic map of the location of the most important sand deserts of the Earth, which we have plotted on Köppen's climatic zones [2], the Selenga

Dauria is confined to the boreal part of the temperate climatic zone. This significantly distinguishes it from classic sand deserts (Sahara, Mojave, Namib and others), which are situated in subtropical and tropical climatic zones (Figure 1). It is worth mentioning that the aeolian sands of the tropics and subtropics are much better studied than the aeolian sands of the temperate climate zone. Previously, the aeolian sands of Selenga Dauria were studied mainly from the perspective of geography, botany and archaeology [3–12]. The problem of the primary source of these sands is still unsolved. Some researchers highlight their direct connection with the aeolian sands of the Gobi Desert [1,3,4], while others believe that they were formed after the Quaternary glaciation [8,10]. In this regard, the main objectives of this study were as follows: (1) to determine the factors influencing the activation of aeolian processes in the boreal zone in the southern part of north Asia; (2) to study the material composition of aeolian deposits and their stratigraphic position (radiocarbon dating) using reference sections; (3) to identify sources of demolition of clastogenic material (origin); (4) to compare the material composition (granulometry, mineralogy) of the studied sands with aeolian sands from subtropical and tropical zones; and (5) to make an environmental assessment of the natural objects discussed in this article. This paper aims at revealing the causes and regularities of desertification development in one of the parts of the boreal zone of northern Asia. This study of the desertification processes in Siberia is crucial due to the development of new land areas in the region.

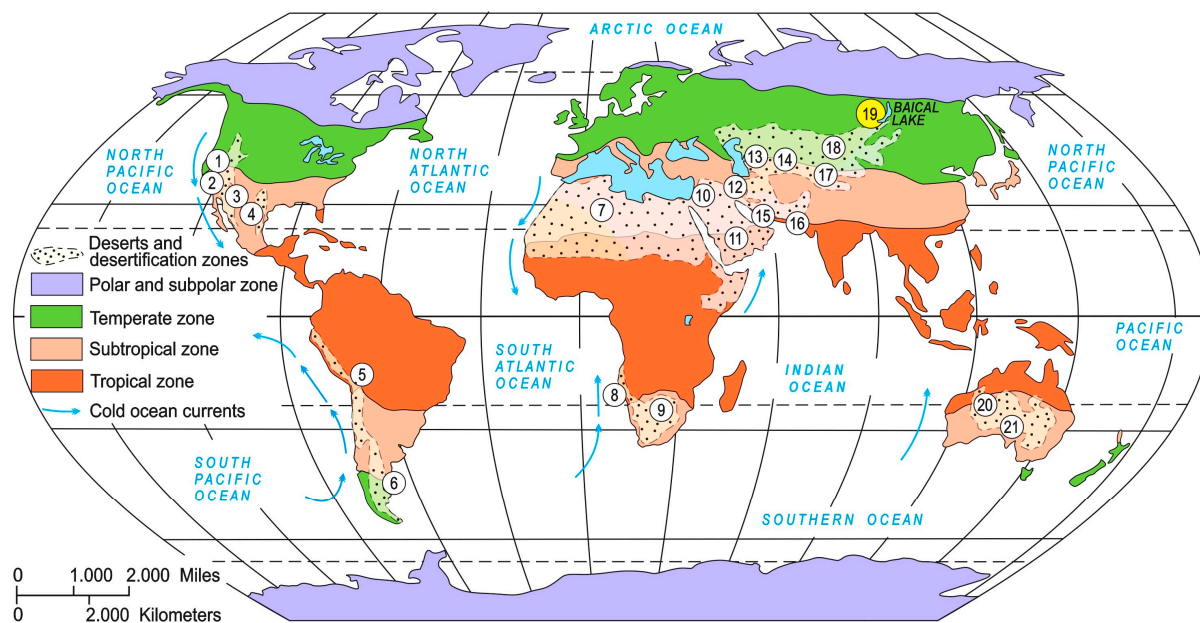


Figure 1. Schematic location map of the most important sand deserts and desertification zones of the Earth against the background of simplified climatic zonation by W.P. Köppen [2]. Figures show the location of the most important deserts and the area of the conducted research: 1—Great Basin, 2—Mojave, 3—Sonora, 4—Chihuahua, 5—Atacama, 6—Patagonia, 7—Sahara, 8—Namib, 9—Kalahari, 10—Syrian, 11—Syrian, 12—Kevir, 13—Karakum, 14—Kyzylkum, 15—Deshte Lut, 16—Thar, 17—Takla Makan, 18—Gobi, 19—Selenga Dauria sands, the area of our research, 20—Australian, 21—Great Victoria Desert. The diagram was drawn up by N.I. Akulov.

In the last decade, the studies of modern aeolian processes and the material composition of sediments, vegetation and landscapes in areas of blown sands have been devoted to the works [9–15]. Information on the distribution of areas of loose sands in the Holocene and the stages of deflation and accumulation is contained in the publications [15–19].

2. Study Area and Methods

It is known that aeolian sands in southern northern Asia are confined mainly to river valleys, hilly plains and intermountain hollows [4–7]. The territory of Selenga Dauria

covers not only Western Transbaikalia but also extends beyond Russia into Mongolia, to the places where the Selenga River originates (Figure 2). An extreme continental semi-arid climate with cold winters and relatively warm summers prevails here. The river valleys and intermountain hollows contain thick (over 30 m) deposits of aeolian strata. Sands largely shape local landscapes represented by pine forests, forest steppes, steppes, semi-deserts and small deserts such as Aman-Khan and Chara. The current progressive desertification of the region significantly aggravates socio-economic and environmental problems. The number of livestock pastures and plowlands is gradually decreasing.

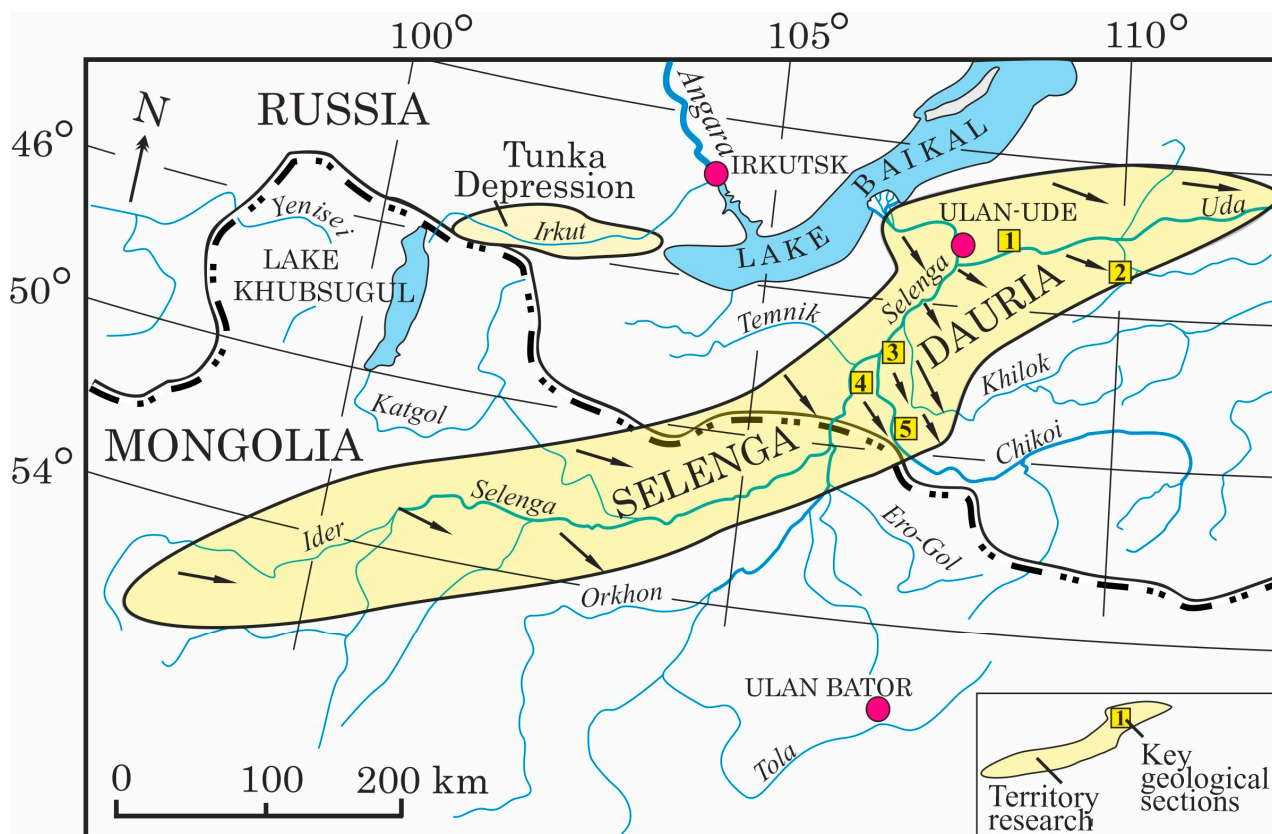


Figure 2. Overview scheme of the region under study 1–5—reference geologic sections: 1—Zaigrayevsky, 2—Ilkinsky, 3—Nomokhonovsky, 4—Debensky, 5—Aman-Khansky. The arrows indicate the prevailing wind directions determined by the elements of aeolian bodies' occurrence (strike). The diagram was drawn up by N.I. Akulov.

Field material was collected in expeditionary work during 2021–2023. Five reference sections were studied, and more than one hundred samples were collected for various types of analyses (Figure 2).

Aeolian fields and dunes were photographed and videotaped over extensive areas using a DJI Air 2S quadcopter. For detailed study of the reference sections, additional mining excavations (pits) and clearings (riverbank bluffs) were carried out. Based on the expedition video footage, an educational video film titled 'In the Aman-Khan Desert' was created [20].

Assessment of the areas of aeolian sand distribution in Selenga Dauria was carried out using the Google Earth Pro software, which allowed us to monitor the development of desertification processes in the period from 1985 to 2020.

The lithological sand analysis included the study of the textural, structural and mineralogical features of the sand. In laboratory conditions, the analyzed 40 g sample was taken by the quartering method from the brought initial sample weighing about 200 g. With the help of bromoform, the analyzed quantity of the sample substance was subjected to division into light and heavy fraction minerals. The obtained fractions were weighed and examined

under the microscope in immersion preparations. To determine the percentage of mineral content, 500 grains from the 0.5–0.25 mm class were randomly selected. The number of grains of each mineral was counted with the initial count of 500 grains considered as 100%. For control of hard-to-diagnose and rare minerals, their X-ray diffraction analysis was conducted using a DRON-3 device. Additionally, the aeolian sands were scrutinized under binoculars for cavernosity, transparency and pelletization.

The grain size distribution of sand sediments was studied by laser diffractometry using the Analysette 22 NanoTec grain size analyzer. The range of determined grain sizes is from 0.08 to 2000 μm . Dispersion of samples was carried out using ultrasound. Sand grains exceeding 2 mm were dispersed on sieves. Grain size distribution histograms (in %) and accumulative curves on a semi-logarithmic scale were constructed based on the studies' findings. The median (Md) and modal (Mo) grain diameters, sorting (So) and asymmetry (Sk) coefficients were calculated for each sample. In addition, the degree of heterogeneity coefficient of the grain size distribution (Kh) was determined.

Radiocarbon dating of the samples was carried out at the St. Petersburg State University and the V.S. Sobolev Institute of Geology and Mineralogy of the Siberian Branch of the RAS by carbon dating of humic acids of buried soils and charcoal [21]. Residual carbon activity was determined using a QUANTULUS-1220 radiometer (Liquid Scintillation Counters from "PerkinElmer Life Sciences/Wallac Oy" company, Finland).

3. Results and Discussion

Detailed field studies were carried out on the Zaigrayevsky, Ilkinsky, Nomokhonovsky, Debensky and Aman-Khansky reference sections (Figure 2).

3.1. Zaigrayevsky

The Zaigrayevsky reference section (Figure 3) is situated in a quarry on the northeastern outskirts of the Zaigrayev settlement. Its main part is confined to the fourth terrace of the Bryanka River. The terrace is composed of horizontally laid light-grey multigrained alluvial sands with gravel lenses, which alternate with layers of aeolian, aeolian-deluvial and deluvial sands. Four horizons of aeolian sands were identified, their thickness varying from 0.2 m to 4.1 m, which indicates frequent changes in facies conditions during formation of the exposed strata. In the upper part of the section, represented by modern aeolian deposits, two horizons of buried soils were revealed, and, in the central part, a bone of a woolly rhinoceros was found [22]. According to the results of earlier studies, woolly rhinoceroses inhabited almost the entire territory of northern Eurasia in the Late Pleistocene [23,24]. Thus, this species is an important biostratigraphic indicator of the Late Pleistocene.



Figure 3. Zaigrayevsky sand quarry (Zaigrayev settlement); GPS: N 51°50'17.0"; E 108°17'41.5".

parameters (modal and median particle diameters, sorting coefficients, asymmetry and heterogeneity) [25,26].

Alluvial sands have a complex bimodal distribution with modes (M_o) in intervals 200–400 μm and 800–1200 μm (Figure 5). In their composition, coarse- and medium-grained classes predominate. These are heterogeneous in composition ($K_n = 6.3$) multigrained sands. Aeolian sands are mainly medium- and fine-grained and are characterized by a single-top ($M_o = 180\text{--}280$ μm), pointed-topped, symmetrical ($S_k = 1.02$) distribution, as well as increased dispersity ($M_d = 200$ μm), homogeneous composition ($K_n = 2.2$) and good sorting ($S_o = 1.48$) (Figure 5). The mixed (aeolian-deluvial) sand type is characterized by a single-top distribution ($M_o = 300\text{--}600$ μm). These are homogeneous ($K_n = 2.9$), moderately sorted ($S_o = 2.48$) sands. They differ from aeolian sands by the presence of coarse-grained material (up to 12%).

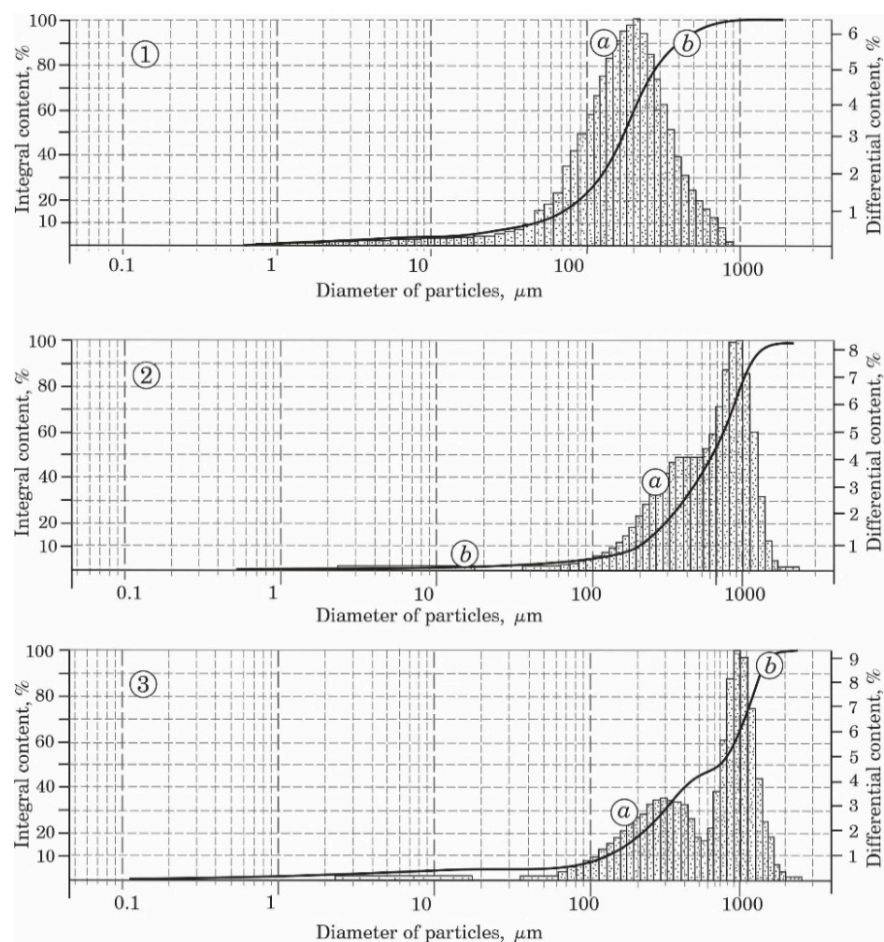


Figure 5. Histograms (a) and accumulative curves (b) of the granulometric composition of the main genetic types of sandy sediments: 1—aeolian (sample 14), 2—mixed (aeolian-deluvial, sample 17) and 3—alluvial (sample 3).

Thus, the studies of the granulometric composition of the layered sandy sediments of the Zaigrayevsky section allowed us to establish that this sandy stratum was formed as a result of repeated change of subaqual accumulation conditions to subaerial ones.

According to the data of mineralogical analysis of the light fraction, all sands of the strata under study have oligomictic quartz–feldspar composition; heavy fraction minerals, which are part of their composition, are represented mainly by amphiboles, epidote, sphene and insignificant amounts (from decimal signs to the first percent) of ilmenite, magnetite, diopside and hypersthene (Figure 4).

3.2. The Ilkinsky

The Ilkinsky reference section is situated 4 km west of Novoiyinsk settlement, on the right bank of the Ilka River. In the northern side of the deflation basin, clearing uncovered a three-meter-high floodplain section with two buried soils and numerous pottery fragments (Figure 6).



Figure 6. Pit at the Ilkinsky reference section. Two soil horizons and numerous pottery fragments buried beneath aeolian sands (pottery is shown in the photo insert, and the arrow shows sands containing pottery); numbers show the calendar age of soil horizons; GPS: N 51° 41' 58.7"; E 108° 37' 26.4".

The section is underlaid by channel gravelites that grade up the section to floodplain coarse-medium grey sands and dark-grey loams overlaid by a pack of alluvial horizontally layered sands. The section is completed by a 1.5-meter-thick massive pack of lighter brownish-yellow aeolian sands containing two horizons of buried soils. Radiocarbon datings were obtained for these (Table 1). Modern aeolian sediments overlie the top buried soil, while older sediments lie between and beneath the fossil soils. Aeolian sediments were found to have accumulated on the floodplain during the Little Ice Age (LIA) of 0.7–0.45 cal. BP and <0.3 thousand years. Apparently, the last stage of sand activation is associated with deforestation, construction of railroads and motor roads, and overgrazing.

Table 1. Radiocarbon and calendar age of sediments of river terraces in the Selenga river basin.

Lab. No	Material	Depth (cm)	14C Age (Years BP)	Calibrated ¹⁴ C Age (cal. Years BP, 2 Sigma Error)	Calibrated Age, Median (cal. Years BP)
Section IL 2. First terrace (4–6 m) of the Il'ka River, 51° 41' 58.2" N, 108° 37' 26.5" E					
SOAN-9859	Humic acid	59–67	275 ± 40	1–463	232
SOAN-9860	Humic acid	87–96	800 ± 180	493–1175	834
Section DB. Fifth terrace (40–45 m) of the Selenga River, 50° 42' 33.18" N, 106° 18' 33.24" E					
LU-10223	Humic acid	124–134	1780 ± 190	1304–2123	1714
LU-10195	Charcoal	210–220	1870 ± 70	1608–1983	1796
LU-10217	Humic acid	388–394	9800 ± 350	10,228–12,468	11,348

Remarks. The radiocarbon dates were converted to calendar dates using Calib Rev 8.1.0 software (calibration curve IntCal20) [27].

The contact between the aeolian sand pack and the underlying alluvial complex is indistinct. The overlying aeolian sand pack is monotonous and lacks layering; its granulometric composition is predominantly fine-grained, and its color is lighter brownish-yellow. According to the mineralogical analysis, the aeolian sands consist mainly of biotite

(up to 48%), feldspars (plagioclase content up to 36.8%, and the amount of kalispars does not exceed 7.2%) and quartz (8%). Higher up the section, the amount of biotite extremely decreases (up to 0.4%), but the content of plagioclase (up to 65.2%) and quartz (up to 24%) increases. Amphibole (up to 56%), magnetite (up to 20%) and sphene (up to 15%) predominate in the composition of the heavy fraction minerals at the base of the aeolian pack. The amount of apatite reaches 5%, and the total content of ilmenite, zircon and epidote does not exceed 4%. In all samples taken higher up the section, the composition of the heavy fraction minerals is relatively stable and is characterized by high content of amphibole (46–54%), sphene (10.4–11.2%), diopside (8–11.2%), epidote (8.8–10.8%), hypersthene (4–8%) and ilmenite (4%). Tourmaline, rutile, zircon and hematite were noted in single decimal signs.

This study of the granulometric composition of the sandy sediments of the Ilkinskiy section was based on the results of analyses of ten samples. Based on comparison of the graphs of clastic particles distribution by fractions, three types of granulometric spectrums were revealed (Figure 7). The first type is represented by fine-grained sands, in the composition of which the content of fine-grained class (0.25–0.1 mm) reaches 53–58% and medium-grained 24–33%. These are homogeneous ($Kn = 2.3–2.5$), well-sorted ($So = 1.48–1.53$) sands. The values of the median diameters (Md) are 180–200 μm . The distribution graphs of their composition are single-top with a slight asymmetry toward coarse dimensions ($Sk = 0.97$). The peculiarity of the granulometric composition of the second type sediments is their diversity: the coarse-grained (1.0–0.5 mm) class is 16%, medium-grained is 39% and fine-grained is 34%. These sands are maximally heterogeneous ($Kn = 2.9–3.16$) and moderately sorted ($So = 1.7–1.75$), with flat-topped distribution ($Sk = 0.83–0.9$). The median diameter of their grains reaches 280–300 μm . Fine-grained sands represent the third type. In their composition, the fine-grained class (0.25–0.1 mm) occupies from 61 to 67%, and the remaining part belongs to close-grained (0.1–0.05 mm) and medium-grained (0.5–0.25 mm) classes in almost equal amounts (15–16%). The sands are homogeneous ($Kn = 2.53–2.59$) and well-sorted ($So = 1.35–1.41$). Values of median diameters (Md) vary from 140 to 170 μm . Distribution plots of their composition are pointed-topped and largely symmetric ($Sk = 1.01–1.03$).

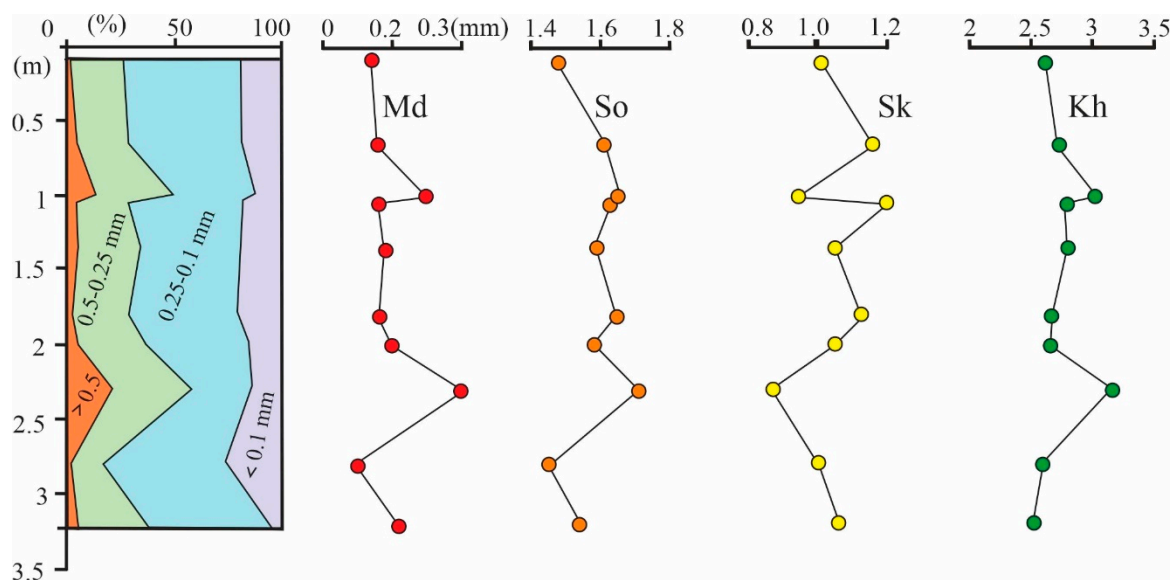


Figure 7. Diagram of granulometric composition and nature of changes in statistical parameters of sands of the Ilkinskiy section (borehole 3-2).

All the above-mentioned parameters indicate that aeolian accumulation occurred rhythmically with a significant activation of the dynamics of the sedimentation environment, which contributed to the inwash of coarse-grained material.

3.3. The Nomokhonovskoye Aeolian Sand Field

The Nomokhonovskoye aeolian sand field is situated on the right bank of the Selenga River, near the settlement of Yekhe-Tsagan (Figure 8). It is represented by ridge blocks whose movement rates reach 2.5 m per year. The dispersed sands come from the Selenga River beach zone and from areas of reweaving of ancient blocks of loess-like deposits.



Figure 8. Nomokhonovsky field of aeolian ridged sands; GPS: N 50°58'40.72"; E 106°22'53.92".

It should be noted that, at the end of the 18th century, the central part of the natural boundary was a home to the Staroye Nomokhonovo settlement that was gradually buried by sands over several centuries. A desert was formed on the sites of the surrounding pastures and meadows. In the beginning of 1934, it was found that about 1/20th of the pasture area was covered with sand [4]. According to land survey data, by 1985, the pasture area had reduced almost to one-fourth of its original size. Currently, the desertification area reaches seven thousand hectares. Monastic chronicles note that the origin of shifting sand pockets began after mass deforestation and became active in the years of disasters caused by drought. Classic aeolian landforms are developed in the area; they are represented by various types of dunes and numerous blowout corridors. The vegetated aeolian and loess sediments of the area, underlying the modern dispersed sands, are united into the Krivoyarskaya suite of the Middle Pleistocene [28]. Their thick covers are found on all northern slopes of the mountain ranges and watersheds, which indicates the centuries-long geologic history of the desertification process. Under the covers of the aeolian sands and loesses of the Krivoyarskaya suite, a horizon of windkanter was uncovered. The suite is represented mainly by fine-grained silty sands with indistinct horizontal layering. It should be noted that, along with aeolian sands, the suite also includes lake-alluvial sediments that were formed during the Samarovskoye glaciation in Western Siberia [29]. The age of the suite, determined based on rhinoceros bones and myospore complex, is limited to the first half of the Middle Pleistocene. The thickness of the suite reaches 90 m.

3.4. The Debensky Reference Section

The Debensky reference section is situated one kilometer west of Deben settlement, on a 45-meter-high ledge of the fifth terrace of the Selenga River (Figure 9). The terrain of the site is hummock-and-hollow, aeolian, with alternating aeolian ridges and deflation basins anchored by herbaceous vegetation. The height differences reach 1 m. Western and northwestern winds carry sand out from the terrace ledge to its surface and form sand ramparts up to 30 cm high.



Figure 9. Debensky reference section; GPS: N 50°42′33.18″; E 106°18′33.24″.

The clearing uncovered sediments of the cover and alluvial genetic complexes. Sediments of the cover genetic complex (5.8 m) include aeolian fine- and close-grained sands and interlayers of poorly humusified sandy loams. A total of six poorly developed soils were identified. Radiocarbon datings were obtained for two of them (Table 1). Short stages of soil formation are associated with the most humid stages of the Holocene. Fragments of a ceramic vessel of Hunnu age (220 BC–2nd century AD) were found 50 m south of the section, in the bottom of the buried soil at a depth of 2.2 m. Thus, during almost the entire Holocene (11.7 thousand cal. years), aeolian close- and fine-grained sands were accumulated (Figure 10).



Figure 10. In the Debensky section, the aeolian deposits are separated by two horizons of buried soils (355 and 428 cm depth). The topsoil horizon has a radiocarbon age of 9800 ± 350 BP (LU-10217).

3.5. Aman-Khan Sand Desert (Mini-Desert)

The Aman-Khan sand desert extends in a submeridional direction 40 km northeast of Kyakhta (Figure 11). The area of sands occupied by the desert is about 15 km^2 , with a length

of more than five kilometers. Some researchers refer to it as the Big Sands natural boundary or the Malkhan-Elysu desert [6,9]. Satellite images show that this is a small sand desert, which is formed not by chaotic piling of parabolic dunes but by their regular succession in the form of transverse sand chains or sand ramparts extending perpendicular to the prevailing wind direction (Figure 12). This is the result of a multi-year cyclic movement of aeolian sands based on rhythmic, predominantly interseasonal, aeolian transportation. It should be noted that parabolic dunes in the marginal parts of the cross-sand ramparts smoothly grade to dome-shaped and vegetated dunes. The base width of some parabolic dunes reaches 160 m, and the length of their symmetry axis is about 80 m.



Figure 11. Aman-Khan sand desert.

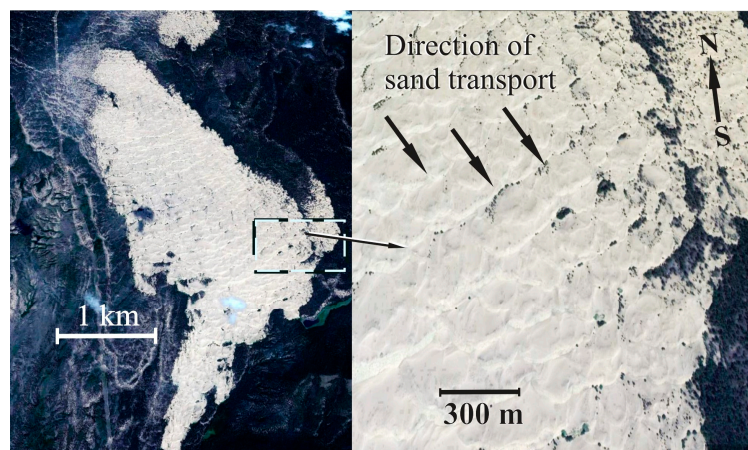


Figure 12. Satellite images of the Aman-Khan desert.

The modern aeolian landforms are well distinguished on satellite images by characteristic channel forms and light coloration of sands.

Transverse sand ramparts represent the main mass of aeolian forms of the Aman-Khan mini-desert (Figure 12). The side slope of each sand rampart is the same as that of a single dune—the windward side is always flat up to 15° , and the leeward side is steep up to 30° . Sand ramparts are always convex in the direction of blowing winds. We identified 46 sand ramparts with an average length of 1520 m, with a width of 30 m and a height of up to 20 m. Their travel rate is 1.5–2.0 m/year. The mineralogical composition of the sands is polymictic, and, by granulometric composition, they are medium and fine-medium grained. Feldspar dominates in the composition of the light fraction minerals, and amphiboles and pyroxenes predominate among the heavy fraction minerals. This indicates a weak chemical maturity of the sand material.

The sand layering is subhorizontal, often indistinctly pronounced. The main element of sand microrelief is aeolian ripple. Superposition of sand grains from the upper parts of the airflow on more active ones in the lower part leads to wave flow interference and formation of aeolian ripple. The movement of the ripple is due to the settling of the leeward slope of the rampart. The aeolian ripple is asymmetric and is observed on almost all surfaces of the observed aeolian forms. The height (amplitude) of the aeolian ripple varies from several millimeters to a few centimeters. The ripple index (the ratio of the ripple wavelength to its amplitude [30]) for the Aman-Khan sands ranges from 23 to 30.

The aeolian sands have a fine- and medium-grained composition, with the content of medium-grained class (0.5–0.25 mm) reaching 48–51% and fine-grained class (0.25–0.1 mm) 41–47%. The distribution of grain size composition is single-top ($M_o = 200\text{--}300\ \mu\text{m}$) and largely symmetrical ($S_k = 0.98\text{--}1.02$). These are homogeneous ($K_n = 2.15\text{--}2.41$), well-sorted ($S_o = 1.41\text{--}1.49$) sands. The median diameter (M_d) values are $240\text{--}280\ \mu\text{m}$ (Figures 13 and 14).

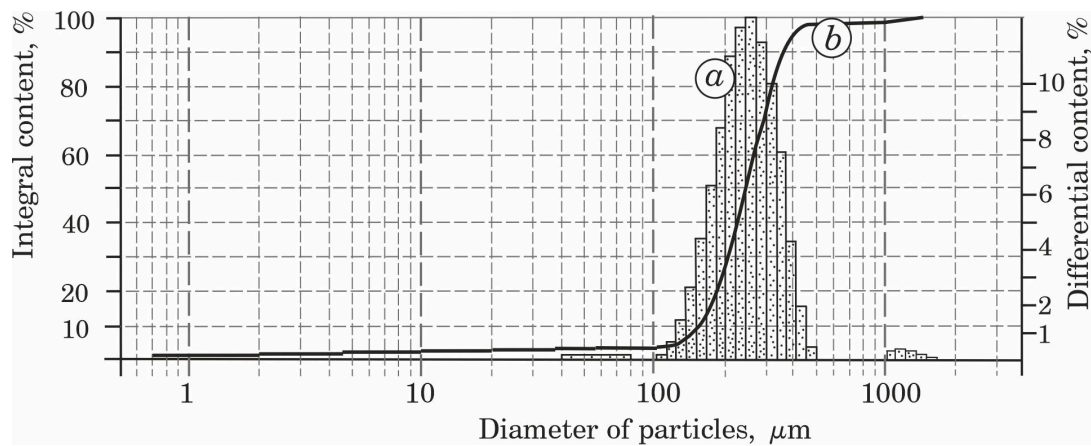


Figure 13. Histogram (a) and integral curve (b) of granulometric composition of aeolian sands in Aman-Khan desert.

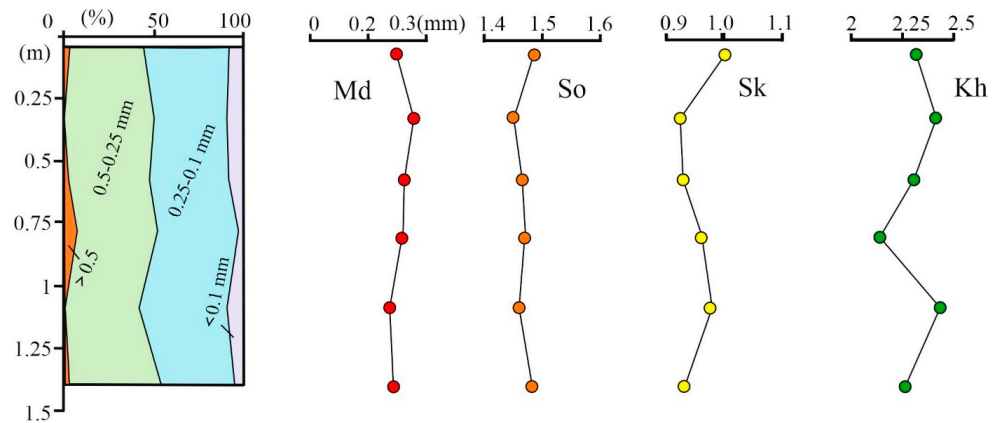


Figure 14. Diagram of granulometric composition and the nature of changes in statistical parameters of the sand strata of the Aman-Khan Desert (borehole 5-1).

Mineralogical sand analysis revealed that their light fraction is dominated by plagioclase (up to 56%), quartz (up to 18%) and potassium feldspar (up to 17%). The heavy fraction is dominated by amphiboles, pyroxenes, magnetite, hematite, ilmenite and serpentine. Their granulometric composition is medium- to fine-grained, with major ratios varying in the following parameters: M_d (0.25–0.3), S_o (1.45–1.5), S_k (0.9–1.0) and K_h (2.1–2.5) (Figures 13 and 14).

R.J. Nicholls and K. Small [31,32] state that most of the Earth’s population is situated within a five-kilometer coastal strip along rivers, lakes and other water bodies where aeolian geosystems are often present. As a result, coastal aeolian geosystems are subject to

intensive anthropogenic impact. The intensification of human activities in the river valleys of Selenga Dauria also contributes to the expansion of desertification zones. Archaeological excavations during the study of aeolian deposits on the shore of Lake Baikal showed that the first ancient human sites were located in the most picturesque places of the lake coastal strip [33]. Ancient human sites of the Neolithic period have been discovered on dune sands along the Ilka (Ilka, Novoilynsk), Ude (Novaya Kurba, Staraya Kurba) and Bryanka (Novaya Bryan) Rivers. The Neolithic era also includes the prehistoric settlement uncovered at the foot of Varvarina Gora (village of Staraya Bryan).

Excavations at the prehistoric settlement of Varvarina Gora [34] revealed four cultural horizons, which developed between 43,000 and 33,000 years BP (horizon 4) and 25,000 to 10,000 years BP (horizon 3). This settlement was inhabited by early hunters of rhinoceroses, wild horses and deer in a slowly drying paleoclimate. A. P. Okladnikov [35] claims the paleogeography of the Ice Age of the Transbaikalia boreal zone is characterized by the abundance of rhinoceros and horse bones but not by the mammoth, which lived much further north in the zone of modern tundra. At younger prehistoric settlements, stone tools and fragments of pottery are confined to the deflation basins, where they, together with buried remains of fireplaces, have been uncovered by pits on the bottoms of the basins or exposed in their walls (Figure 10). Deflation basins have an elliptical shape in plan view, stretched along the direction of prevailing winds. The depth of such basins reaches 15 m, while their length can extend up to 300 m.

Deflationary trails, rills, grooves and blowout corridors occur on dense loamy and clayey surfaces at the bottom of dried lake basins or alluvial plains. Blowout corridors, unlike those we studied on the Lake Baikal shores [36], are rectilinear, are always oriented in the direction of the prevailing winds, have steep slopes and extend up to several hundred meters in length, with a width of several tens of meters and a depth of up to 15 m. We noted that, around the Nomokhonovo natural boundary, active formation of the sand complex began in the Middle Pleistocene (Krivoyarskaya suite).

To assess the degree of development of aeolian processes in the region, we calculated the desertification coefficient (K_d), which is equal to the ratio of the total area of dispersed sand covers in the hollow (S_d) to the area of the hollow itself (S_c), expressed in percent [8].

$$K_d = \frac{S_d}{S_c} \times 100\%$$

Calculations have shown that at present the desertification coefficient in Selenga Dauria is 14.7%, while, in the Tunkin rift valley, it does not exceed 0.8%.

The activation of aeolian activity in the Middle Pleistocene was associated with the intensification of geodynamic processes and changes in wind patterns in the region. According to P. Hesp [37] and J. Young et al. [38], there is a dependence of aeolian geosystems on the modern geodynamics of the territory where they are located. According to the researchers, effective management of the aeolian geosystem requires identifying the predominant types of geological wind activity and monitoring their development in real time.

Analysis of geodynamic activity of the studied area showed that it is located in the zone of stable crustal uplift caused by the convergence of the Amur Plate with the block structures of the Kazakh Shield [39,40]. Recent measurements using GPS geodesy have confirmed the tectonic inheritance of current vertical movements, which vary from 2.6 to 3.2 mm/year [41].

All strong earthquakes that occurred in the Selenga Dauria zone over the last millennium have contributed to regional thickening of the Earth's crust and to uplift of its surface. Such uplift in the western United States is believed to have caused the worst multi-year drought [42].

The slow uplift of the Selenga Dauria resulted in the submergence of groundwater and drainage of the area. A gradual desertification of the region began, accompanied by increased wind activity. The extreme continental climate of the temperate zone during the transition period between seasons (winter to spring) promotes intensive circulation of air

masses, which leads to prolonged and stormy winds. Currently, the average amount of atmospheric precipitation calculated from the meteorological database of such cities as Ulan-Bator and Ulan-Ude is about 250 mm/year, which corresponds to the humidity of the semi-arid desert climate. The active wind regime contributes to soil desiccation, deflation and the formation of aeolian landforms. Aeolian ripples always reflect the intensity of the wind regime. In flat areas of aeolian sand accumulation, the aeolian ripple extends wavelike, with a displacement rate of about 1.6 m/year.

Analysis of wind direction using satellite images demonstrated that the primary aeolian train of sand material was from the Selenga River and other rivers (Figure 15). As a result, the aeolian sand accumulation is completely unrelated to wind activity in the Gobi Desert. Thus, the geological work of winds in the territory of Selenga Dauria involves the removal of sandy silty grains from the river beach and terrace zones, dried-up river-formed lakes and floodplains and their transportation to the desertification zones.

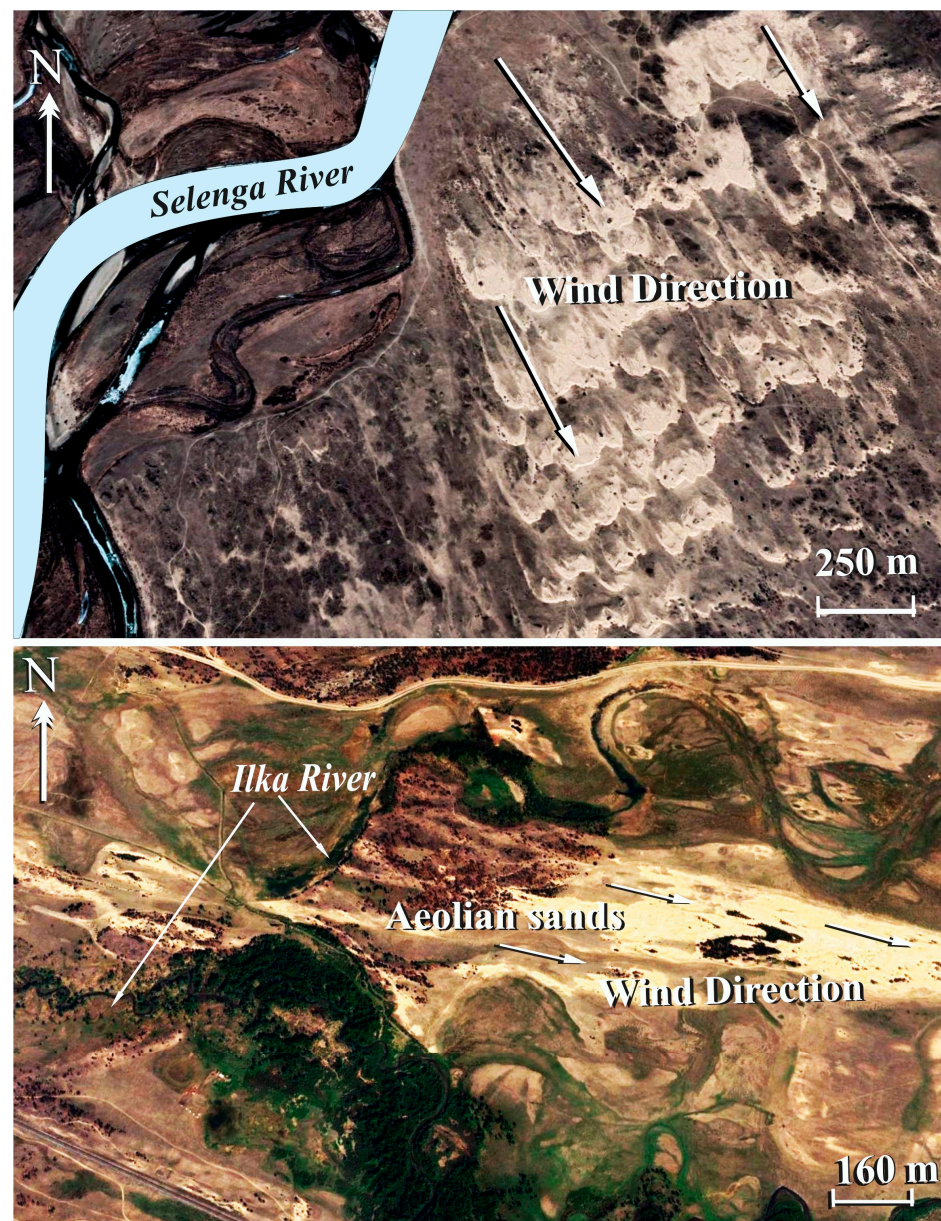


Figure 15. The aeolian sand flows are carried out from the zones of river beaches, dried-up river-formed lakes and floodplains to the desertification zones.

Based on the classical works of H.E. Reineck and I.B. Singh [43], as well as K. Paya and H. Tsoarom [44] on the study of aeolian sediment morphology, we found that the studied sand fields are represented mainly by transverse aeolian ramparts consisting of different types of dunes: parabolic, dome-shaped and vegetative.

We should emphasize that, in the boreal forests and forest steppes of the marginal part of the Tunkin rift valley, lying and vegetative dunes are predominantly distributed. In its middle steppe part, aeolian deposits are laid down in the form of dome-shaped dunes—sand mounds. The mounds' diameter reaches 75 m, their height is about 3 m, and their distance from each other is up to 0.5 km. One of the mounds opened by a pit to a depth of 1.9 m is composed of indistinctly laminated light-grey medium- and fine-grained sands [8].

Parabolic dunes are the most interesting and a very common type of dune, confined exclusively to the Selenga River coast. Sand carried by strong winds from the Selenga River beach zone undergoes differentiation of clastogenic material in the airflow. It was found that in the transportation zones the wind gust velocity decreases and gravitational deposition of the heaviest minerals and their debris occurs. Usually, the transportation zone is located several hundred meters away from the beach and covers an area of up to several hundred square meters, extending along the coastline. It is here that repeated sorting of aeolian sediments takes place, manifested in their intensive reweaving in the near-surface layer and the transport of sands by wind gusts to the dune edges.

The results of granulometric analysis of aeolian sands carried out on all reference sections of Selenga Dauria showed that they are predominantly medium- and fine-grained and well-sorted. The number of medium-grained grains in their composition reaches 70%, and the remaining part is composed of fine-grained material.

In assessing the overall mineralogical composition of aeolian sands of Selenga Dauria, we should note that plagioclase, potassium feldspar and quartz dominate in the light fraction, while the heavy fraction is characterized by amphibole, pyroxene, magnetite, hematite, ilmenite and serpentine.

A comparative analysis of the granulometric composition of the sands we studied and those of contemporary deserts revealed a significant difference between them. L.B. Rukhin [45] claims that the Karakum desert sands are composed predominantly of sand grains ranging in size from 0.25 to 0.05 mm, the sands of the Takla-Makan desert range from 0.25 to 0.10 mm, and the sands of the Indian deserts are characterized by approximately the same content of granulometric classes 0.20–0.16 mm, 0.16–0.11 mm and 0.11–0.08 mm. It is noted that the sands from the relatively nearby Gobi Desert are classified as fine-grained in terms of granulometric composition, with fine-grained material constituting up to 72%, and the remaining portion predominantly consisting of medium-grained particles, up to 22%.

Mineralogical analysis of sands from the northern part of the Gobi Desert differs significantly from the sands of Selenga Dauria. Quartz (up to 64%), plagioclase (up to 27%) and potassium feldspar (up to 8%) dominate in the composition of their light fraction minerals. Among the heavy fraction minerals are ilmenite (up to 25%), sphene (up to 22%), garnets (up to 19%), magnetite and epidote (up to 7%) and amphiboles and hematite (up to 4%), and the total amount of zircon, leucoxene, goethite and pyroxenes reaches 8%.

The Sahara Desert aeolian sands (near Tozer) have a significant difference. Their granulometric composition is characterized by a predominance of fine- and close-grained classes (with 63.7% in the 0.1–0.05 mm class and 30.7% in the 0.25–0.1 mm class). Additionally, they contain a wide range of weathering-resistant minerals, including quartz, leucoxene, ilmenite, epidote, zircon, garnets, tourmaline, rutile and sphene (according to the scale proposed by R.K. Selley [46]).

In contrast, the mineral grains constituting the sands of the Selenga-Dauria region exhibit relatively low stability, as they are predominantly composed of minerals that are less resistant to weathering, such as plagioclase, feldspar, amphibole and pyroxene.

4. Conclusions

1. The activation of aeolian processes in the boreal zone of southern north Asia is determined by a complex interaction of natural and anthropogenic factors. Natural factors include the positive influence of recent neotectonic movements; wide distribution of alluvial and lake-alluvial deposits in river valleys and hollows; an extreme continental semi-arid climate; strong winds in spring and summer; uneven seasonal and long-term distribution of precipitation; and forest steppe and steppe vegetation. Among anthropogenic factors, the leading ones are deforestation, land plowing and construction of line structures.

2. The study of the reference section sediments and radiocarbon dating of buried soils indicate the active manifestation of deflation and accumulation processes in the Holocene. Aeolian processes were most active during the cold epochs (cryochrons) of the Pleistocene and Holocene. In the Pleistocene warming epochs (thermochrons) and in the Holocene, deflation and accumulation of sands alternated with stages of pedogenesis.

3. The primary sources for aeolian transportation are floodplains and river terraces composed of sandy sediments. Aeolian sands were formed as a result of nearby wind transportation. Areas of deflated and drifting sandy sediments are distinguished. They form mini-deserts non-fixed by vegetation, with active aeolian processes, barchans, dunes, and deflationary basins. Aeolian landscapes poorly fixed by vegetation are characterized by ridges and deflationary basins.

4. Aeolian sediments of the boreal zone of northern Asia, in contrast to similar sands of subtropical and tropical zones, consist of coarser-grained material. They are dominated by medium- and fine-grained sands, which are polymineral and well-sorted. In subtropical and tropical deserts, aeolian sands are typically monomineral and consist of fine- and very-fine-grained particles.

5. The mineralogical composition of the studied aeolian sands is represented mainly by minerals unstable to weathering (feldspars, plagioclases, pyroxenes and amphiboles). Quartz, leucoxene, ilmenite, epidote, zircon, garnets, tourmaline, rutile and other stable minerals dominate in the sands of classical deserts.

6. Modern aeolian landscapes are a unique natural formation of the boreal zone of northern Asia. They are widely spread in the Republic of Sakha (Yakutia) and in Western and Eastern Siberia. Aeolian landscapes can be used for the development of ecotourism.

Author Contributions: Conceptualization, N.A.; formal analysis, V.A., M.R. and Y.R.; investigation, N.A., Y.R. and M.S.; resources, V.A. and M.R.; data curation, Y.R. and M.S.; writing—original draft preparation, N.A. and V.A.; writing—review and editing, Y.R., M.S. and V.A.; visualization, V.A. and Y.R.; supervision, Y.R.; project administration, Y.R.; funding acquisition, N.A. All authors have read and agreed to the published version of the manuscript.

Funding: This research received no external funding.

Data Availability Statement: The data are contained within this paper.

Conflicts of Interest: The authors declare no conflicts of interest. The funders had no role in the design of this study; in the collection, analyses or interpretation of data; in the writing of the manuscript; or in the decision to publish the results.

References

1. Obruchev, V.A. The shifting sands of the Selenga Dauria and the need for their rapid study. In *Proceedings of the Troitskosavsk-Kyaktinsky Branch of the Amur Department of the Imp. Russian Geographical Society*; Publishing House "Saint Petersburg: Senate Printing House": St. Petersburg, Russia, 1914; Volume 15, pp. 1–18.
2. Köppen, V. *Fundamentals of Climatology (Climates of the Earth)*; Tikhomirov, E.I., Ed.; Publishing House of NARKOMPROSA RSFSR: Moscow, Russia, 1938; pp. 1–257.
3. Bazarov, D.B. On the development of blowing sands in the Selenga-Khilok interfluvium and measures to combat them. In *Book: Materials on the Study of the Productive Forces of the Buryat-Mongolian Autonomous Soviet Socialist Republic*; Buryat book publishing house: Ulan-Ude, Russia, 1957; Volume 3, pp. 555–564.
4. Ivanov, A.D. *Aeolian Sands of Western Transbaikalia and Cisbaikalia*; Buryat book publishing house: Ulan-Ude, Russia, 1966; pp. 1–230.

5. Szczypek, T.; Vika, S.; Snytko, V.A.; Buyantuev, A.B. *Facies of Blowing Sands of the Chikoy-Selenga Interfluve in Western Transbaikalia*; Publishing House of the Institute of Geography SB RAS: Irkutsk, Russia, 2000; pp. 1–71.
6. Szczypek, T.; Vika, S.; Snytko, V.A.; Ovchinnikov, G.I.; Namzalov, B.B.; Dambiev, E.T. *Aeolian Tract Mankhan-Elysu in Transbaikalia*; Publishing House of the Institute of Geography SB RAS: Irkutsk, Russia, 2005; pp. 1–61.
7. Vyrkin, V.B. Aeolian relief formation in the Baikal region and Transbaikalia. *Geogr. Nat. Resour.* **2010**, *3*, 25–32.
8. Akulov, N.I.; Rubtsova, M.N. Aeolian deposits of rift zones. *Quat. Int.* **2011**, *234*, 190–201. [[CrossRef](#)]
9. Dulepova, N.A.; Korolyuk, A.Y. Vegetation of blowing sands and sandy steppes in the lower part of the river basin. Selenga (Republic of Buryatia). *Veg. Russ.* **2015**, *27*, 78–95. [[CrossRef](#)]
10. Bazhenova, O.; Kobylkin, D.; Tyumentseva, E. Aeolian Material Migration in Transbaikalia (Asian Russia). *Geosciences* **2019**, *9*, 41. [[CrossRef](#)]
11. Chernykh, V.N.; Tsydyrov, B.Z.; Sodnomov, B.V.; Ayurzhanayev, A.A.; Zharnikova, M.A.; Gurzhapov, B.O. The current state of the landscapes of the blowing sands of the Selenga-Chikoy interfluve (the central part of the Selenga midlands). *Adv. Mod. Nat. Sci.* **2020**, *12*, 163–168.
12. Akulov, N.I.; Rubtsova, M.N.; Akulova, V.V.; Shchetnikov, A.A. Phenomenon for the modern ferromanganese mineralization in aeolian sediments along the coastal zone of Lake Baikal (Siberia). *J. Earth Syst. Sci.* **2022**, *131*, 20. [[CrossRef](#)]
13. Enikeev, F.I. Peski Urotshistshe in the Charskaya Depression (Northern Transbaikalia). *Geogr. Nat. Resour.* **2014**, *35*, 352–358. [[CrossRef](#)]
14. Kobylkin, D.V.; Golubtsov, V.A.; Batozyrenov, E.A. The Dynamics of aeolian morphogenesis in the central part of the Selenga middle mountains. *Bull. Irkutsk State Univ. Ser. Earth Sci.* **2017**, *20*, 43–52.
15. Golubtsov, V.A.; Ryzhov, Y.V.; Kobylkin, D.V. *Late Glacial and Holocene Soil Formation and Sedimentation in the Selenga Middle Mountains*; Publishing House of Institute of Geography SB RAS: Irkutsk, Russia, 2017; 139p.
16. Kobylkin, D.V.; Vyrkin, V.B.; Frolov, A.A. Development of sand landscapes of the western part of the Malkhan range (Western Transbaikalia). *BSU Bull. Biol. Geogr.* **2019**, *4*, 41–54. [[CrossRef](#)]
17. Kobylkin, D.V.; Vladimirov, I.N.; Vyrkin, V.B.; Vershinin, K.E. Dynamics of vegetation cover of Southwestern Transbaikalia in the Holocene (a case study of Malkhanskii range). *Geogr. Nat. Resour.* **2020**, *55*, 141–146. [[CrossRef](#)]
18. Budaev, R.T.; Kolomiets, V.L. Features of Aeolian Relief Formation in the South-Eastern Baikal Region and Western Transbaikalia. Geographical Studies of Siberia and the Altai-Sayan Transboundary Region: Materials of the International Scientific and Practical Conference. Ph.D. Thesis, Altai State University, Barnaul, Russia, 2021; pp. 112–125.
19. Bazhenova, O.I.; Tyumentseva, Y.M.; Cherkashina, A.A.; Tukhta, S.A. *Exogenous Relief Formation in Dauria Steppes*; Publishing House of Siberian Branch RAS: Novosibirsk, Russia, 2023; 181p.
20. Akulov, N.I. In the Aman Khan Desert. Video. Available online: <https://youtu.be/UguQ6YHkACE> (accessed on 14 February 2024).
21. Wagner, G.A. *Scientific Dating Methods in Geology, Archeology and History*; Tekhnosphere: Moscow, Russia, 2006; Volume 534, ISBN 5-94836-037-7.
22. Budaev, R.T.; Kolomiets, V.L. Sedimentary strata of the Gusinozersk-Uda branch of the intermountain depressions of Western Transbaikalia in the Neopleistocene (lithology, genesis and paleogeography). *Domest. Geol.* **2013**, *3*, 47–54.
23. Boeskorov, G.G. Woolly rhino (*Coelodonta antiquitatis*) distribution in Northeast Asia. *Deinsea* **2001**, *8*, 15–20.
24. Novgorodov, G.P.; Boeskorov, G.G.; Cheprasov, M.Y. Preliminary data on cranio- and osteometry of the woolly rhinoceros from the Irilyakh-Siene locality (middle reaches of the Kolyma River). *NEFU Bull.* **2018**, *5*, 44–53. [[CrossRef](#)]
25. Trask, P.D. *Origin and Environment of Source Sediments of Petroleum*; Gulf. publ. Co.: Houston, TX, USA, 1932; pp. 1–281.
26. Lomtadze, V.D. *Physical and Mechanical Properties of Rocks*; Subsoil: Leningrad, Russia, 1990; pp. 1–327.
27. Reimer, P.J.; Austin, W.E.N.; Bard, E.; Bayliss, A.; Blackwell, P.G.; Bronk Ramsey, C.; Butzin, M.; Cheng, H.; Edwards, R.L.; Friedrich, M.; et al. The IntCal20 Northern Hemisphere radiocarbon age calibration curve (0–55 calkBP). *Radiocarbon* **2020**, *62*, 725–757. [[CrossRef](#)]
28. Taisaev, T.T.; Turunkhaev, D.V.; Plyusnin, A.M. Ecological and geochemical features of the Karian gold-bearing region. *Bull. Buryat State Univ.* **1997**, *1*, 113–145.
29. Bazarov, D.B.; Ivanov, A.D. *Shifting Sands of the Buryat-Mongolian Autonomous Soviet Socialist Republic and Measures to Combat Them*; Buryat book publishing house: Ulan-Ude, Russia, 1957; pp. 1–84.
30. Botvinkina, L.N. *Methodological Guide to the Study of Layering*; Science: Moscow, Russia, 1965; pp. 1–260.
31. Nicholls, R.J.; Small, C. Improved estimates of coastal population and exposure to hazards. *EOS* **2002**, *83*, 301. [[CrossRef](#)]
32. Small, C.; Nicholls, R.J. A global analysis of human settlement in the coastal zone. *J. Coast. Res.* **2003**, *19*, 584–599.
33. Akulov, N.I.; Agafonov, B.P.; Krasnoshchekov, V.V. Aeolian deposits covering ancient human sites (Baikal region). *Lithol. Miner.* **2008**, *2*, 209–222.
34. Zhumashov, A.P. *Ecological and Geographical Conditions and Types of Deserts in Central Asia*; Ylym: Ashgabat, Turkmenistan, 1990; 314p.
35. Okladnikov, A.P. *Archeology of North, Central and East Asia*; Science: Novosibirsk, Russia, 2003; 663p.
36. Akulov, N.I.; Agafonov, B.P. Aeolian sands on Baikal and their connection with ilmenite placers. *Reg. Geol. Metallog.* **2005**, *23*, 132–138.
37. Hesp, P. Foredunes and blowouts: Initiation, geomorphology and dynamics. *Geomorphology* **2002**, *48*, 245–268. [[CrossRef](#)]

38. Yang, Y.; Guan, C.; Hasi, E. Dynamic Changes of Typical Blowouts Based on High-Resolution Data: A Case Study in Hulunbuir Sandy Land, China. *Math. Problems Eng.* **2017**, *2017*, 9206963. [[CrossRef](#)]
39. Sherman, S.I. *Modern Geodynamic Zoning of Central Asia as a Leading Factor in the Localization of Strong Earthquakes; Modern Geodynamics of Central Asia and Hazardous Natural Processes; Results of Studies on a Quantitative Basis*: Irkutsk, Russia, 2016; pp. 64–66.
40. *Map of Modern Vertical Movements of the Earth's Crust Based on Geodetic Data on the Territory of the USSR (SVDZK)*. Scale 1: 5,000,000; Pogorazdova, S.V., Ed.; Factory 11 PO "Azerbaijan Aerogeodesy" GUGK USSR: Baku, Azerbaijan, 1989.
41. Sankov, V.A.; Lukhnev, A.V.; Miroshnichenko, A.I.; Perevalova, N.P.; Dobrynina, A.A.; Sankov, A.V.; Lebedeva, M.A. Contemporary vertical crustal movements of Baikal region: Long-term trends and time variations. In *Book: Current Problems of Science in the Baikal Region*; Publishing House SB RAS: Irkutsk, Russia, 2017; pp. 181–187.
42. Borsa, A.A.; Agnew, D.C.; Cayan, D.R. Ongoing drought-induced uplift in the western United States. *Science* **2014**, *345*, 1587–1590. [[CrossRef](#)]
43. Reineck, H.-E.; Singh, I.B. *Depositional Sedimentary Environments*; Springer: Berlin, Germany; New York, NY, USA, 1980; 549p.
44. Pye, K.; Tsoar, H. *Aeolian Sand and Sand Dunes*; Unwin Hyman: London, UK, 1990; 396p.
45. Rukhin, L.B. *Basics of Lithology*; Nedra: Leningrad, Russia, 1966; 703p.
46. Selley, R.C. *An Introduction to Sedimentology*; Academic Press: London, UK, 1976; 408p.

Disclaimer/Publisher's Note: The statements, opinions and data contained in all publications are solely those of the individual author(s) and contributor(s) and not of MDPI and/or the editor(s). MDPI and/or the editor(s) disclaim responsibility for any injury to people or property resulting from any ideas, methods, instructions or products referred to in the content.